A Li-ion Battery Charger Based on Remaining Capacity with Fuzzy Temperature Control

Bo-Ruei Peng
Dept. of E.E., NTUST
Taipei, Taiwan

Shun-Chung Wang*
Dept. of E.E., LHU
Taoyuan, Taiwan
wangsc@mail.lhu.edu.tw

Yi-Hua Liu
Dept. of E.E., NTUST
Taipei, Taiwan
yhliu@mail.ntust.edu.tw

Yan-Syun, Huang
Dept. of E.E., LHU
Taoyuan, Taiwan

***Abstract*—Using high C-rate currents to charge batteries will cause large electrochemical reaction stresses, and thus result in high temperature rise and aggravate battery aging. To alleviate the battery aging and extend the life cycle, a remaining capacity (RC) charge method with fuzzy temperature control is proposed in this paper. According to the derived relationship between the charge C-rate and the state of charge (SOC) of the battery, a corresponding coarse-tuning charge current is determined. To control the temperature rise for subduing the aging effect, a fuzzy temperature controller (FTC) is designed to generate an incremental charging current to fine adjust the charge current. Following the charging progresses, by combining the fine-tune current with the coarse-tuning current, the studied charger can provide the adaptive charge current to charge the battery at any time. The synchronous-rectified buck converter is utilized to implement the charger. The firmware of the adaptive RC charging algorithm is realized by a microcontroller unit. Experimental results are given to verify the correctness and effectiveness of the proposed approach. Comparing to the conventional constant current-constant voltage (CC-CV) method, the proposed charging method reduces 23.2% of average temperature rise and increases 2.06% charge efficiency while maintaining similar charging time.**

Keywords—fuzzy logic control; lithium ion battery; remaining capacity; state of charge (SOC)

I. Introduction

The secondary (rechargeable) batteries play a significant role in energy storage solutions in the modern battery-powered technologies. Proliferation of portable mobile communication devices leads to the demand of rechargeable batteries with different capacities and cell chemistries increasingly. Among the commonly used secondary batteries, the lithium-ion (Li-ion) batteries are a popular choice for applications in various electronic appliances, e.g. hand-held consumer electronics, aerospace, transportation vehicles, and energy backup for renewable energy systems etc. The Li-ion battery features attractive characteristics like more environmentally friendly, high energy and power density, high open-circuit voltage (OCV), low self-discharge rate, less maintenance, and immunization of memory effect [1]-[3].

However, the Li-ion batteries are highly sensitive to deep discharge or overcharge on account of the unsuitable charge or discharge current. As a result, how to make safe and rapid charging achievable, however still maintain high efficacy has become a focus and challenge of charger development [4]–[6]. The constant current–constant voltage (CC-CV) is the most widely adopted charging method for commercial Li-ion batteries nowadays [7], [8], it can achieve the most capacity charge. Nevertheless, the battery temperature rise in the CC phase is high, and the CV charging phase substantially prolongs the charging time and also degrades the charging efficiency. In [9]-[12], Chen et al. addressed a series of improvements in charging strategies, waveforms, or circuit topologies to meet the requirement of fast charging. These methods and schemes indeed improved charging efficiency and speed. The advantages of the multistage CC-charging methods, including less chemical reaction stress and shorter charging time, have been confirmed in [13]-[15]. Recently, the intelligent control algorithms, such as fuzzy control, neural network, genetic, and particle swarm optimization (PSO) approaches [16]-[18], have also been realized by microcontrollers to enhance the charge efficiency and operating performance of the charger.

The available functionality and lifetime of the Li-ion batteries are intensely related to their electrochemical characteristic, operating temperature, and depth of discharge. The pursuit of fast charge causes charge current must be boosted and thus leads to the increase of the battery temperature. The temperature rise makes a significant impact on the battery's life expectancy during charging phase. The higher the temperature rise represents the larger stress of the electrochemical reaction, the faster aging, the higher power loss, and the lower charging efficiency and, can also cause safety concerns. Therefore, a Li-ion battery charger that can provide adaptive charging currents on different conditions is proposed in this paper. The remaining capacity (RC) with fuzzy temperature control is devised to limit the battery temperature rise, alleviate the battery aging and extend the life cycle. A coarse-tune charging current is determined according to the relationship between the charge current and the present battery's SOC. A fuzzy temperature controller (FTC) is designed to generate a fine-tune incremental charging current. The desired adaptive charge current, which features ability of temperature rise control, is produced by adding the fine-tune incremental current to the coarse-tune current. The implementations of the hardware and firmware were described in detail. Experimental results are measured and comparisons with the conventional counterparts were also included to

978-1-5090-0806-3/16/$31.00 copyright 2016 IEEE
ICIS 2016, June 26-29, 2016, Okayama, Japan

validate the correctness and effectiveness of the proposed approach.

II. Proposed Charger Architecture

A. System Configuration

Fig. 1 shows the hardware of the proposed digitally-controlled Li-ion battery charger. The input voltage of the charger derived from an adapter with 24V output voltage. The battery pack with power management ICs used for general notebooks is made up of 4-series-2-parallel (4S2P) cells. The rated voltage of the pack is 16.8V, and all cells are screened beforehand to ensure that each cell has the similar characteristics (e.g. the similar internal impedance and open circuit voltage). The synchronous buck converter was adopted as the power stage. The gas gauge IC BQ20Z45 was used to estimate the SOC of the battery pack. The temperatures of the battery exterior and room were detected by the thermocouple input module NI 9211. The RC charge method was implemented by the dsPIC microcontroller. The fuzzy temperature rise control was realized in the PC using LabVIEW program. The firmware written in the microcontroller carries out the RC charging strategy and quantizes the sensed voltage, current, SOC, and feedback signals to reduce the circuit complexity. The graphic user interface (GUI) records and monitors various battery data and waveforms during the charge process. The SOC gauge IC communicates with the microcontroller through the inter-integrated circuit (I^2C) protocol. The connection between the microcontroller and PC is the RS-232.

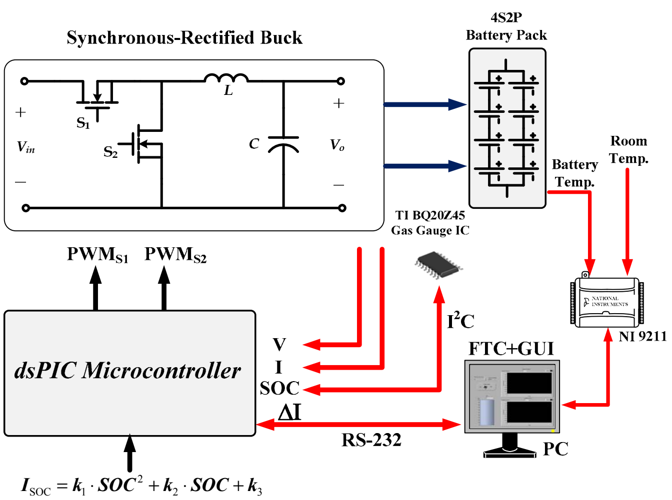

Fig. 1. Charger configuration.

Through I^2C, the acquired information from the gauge IC, including the SOC and battery's voltage and current, is read by the microcontroller. These data are also transmitted to the GUI via the RS-232. According to the derived relationship between the charge current and battery's SOC, a corresponding coarse-tuning charge current I_{SOC} is determined based on the RC charge strategy in the microcontroller. The thermocouple input module NI 9211 measures the room temperature and battery surface temperature. The acquired temperature data are sent to the fuzzy temperature controller (FTC) which is realized in the PC by the LabVIEW software. Based on the variation of the temperature, the FTC outputs a fine-tune incremental charging current ΔI (may be a positive or negative value). Then coarse-tuning charge current can be modified by the incremental charging current to generate the desired adaptive charge current, which features ability of temperature rise control.

B. RC Charging Strategy

Using high C-rate currents to charge high remaining SOC (RSOC) cells will result in high temperature rise and aggravate the battery aging due to the large stress of the electrochemical reaction. Accordingly, the relevant data during battery charge and discharge were recorded and the relationship between the charging current and the SOC can be extracted. To alleviate aging effect and extend the lifetime, the charger can provide a safe current corresponding to the present SOC status to charge the battery. Therefore, to obtain the relationship between the SOC and the charge current, the battery pack with various RSOCs was charged to full capacity by the different C-rate. Table I shows the required charge time (CT) for the battery with various RSOCs charged by different C-rate currents. The temperature variation for the battery at the same test condition was shown in Fig. 2.

TABLE I. Measured Required CT

SOC \ I_{ch}	0.2C	0.3C	0.4C	0.5C	0.6C	0.7C	0.8C	0.9C	1C
0%	5:33:27	4:00:21	3:13:28	2:42:03	2:25:16	2:12:11	2:03:30	1:56:07	1:50:30
10%	5:03:58	3:41:56	3:00:16	2:21:46	2:17:17	2:05:20	1:57:13	1:52:29	1:46:59
20%	4:33:35	3:19:46	2:44:08	2:20:43	2:07:27	1:57:02	1:49:03	1:48:13	1:40:52
30%	3:53:20	2:58:44	2:28:44	2:08:06	1:56:07	1:47:50	1:43:19	1:39:28	1:33:59
40%	3:31:53	2:39:06	2:01:51	1:55:18	1:46:17	1:38:03	1:34:41	1:32:13	1:27:17
50%	2:51:33	2:18:56	1:46:38	1:42:59	1:34:56	1:30:01	1:27:18	1:24:13	1:21:02
60%	2:31:39	1:56:43	1:38:25	1:29:57	1:25:13	1:20:38	1:18:41	1:16:50	1:13:52
70%	1:49:32	1:32:58	1:22:33	1:15:43	1:11:51	1:08:46	1:07:49	1:04:57	1:04:28
80%	1:24:13	1:10:04	1:04:05	0:58:36	0:57:41	0:54:27	0:54:18	0:54:14	0:53:07
90%	0:52:21	0:47:01	0:44:27	0:42:39	0:42:12	0:42:00	0:41:50	0:41:45	0:41:38

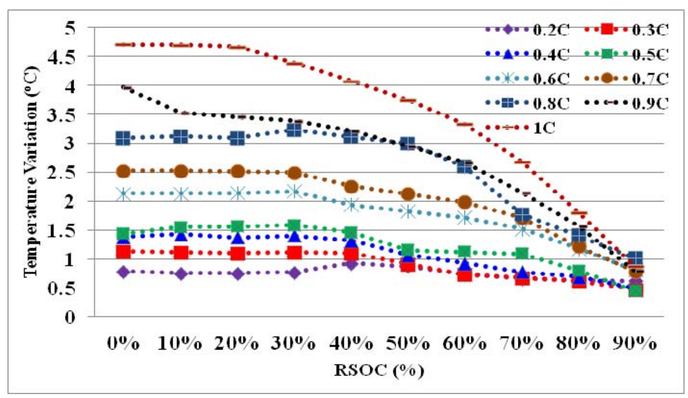

Fig. 2. Temperature variation.

From Table I, taking the CT of the 1C as the numerator and the CT of the 0.2C~0.9C as the denominator, then we can obtain the CT ratio of the 1C versus 0.2C~0.9C under different RSOC as shown in Table II. In order to shorten the charging time but still maintain the acceptable temperature rise, more than 0.9 CT ratios (coloring fields) are chosen in this study. Hence, from the connection between the RSOC and charging current (Table I) and the impact of the charge current on the temperature rise (Fig. 2), the suitable charge C-rate for a battery with different SOC can be found, as shown in Table III. Where the I_{bat} in Table III is the charge current at 1C. The selected charge current is the coarse-tune current (I_{SOC}) in this research. It can effectively subdue the temperature rise and has the CT approaching to that of the 1C charge current. In addition, a mathematical model is built from the limited experimental samples to fulfill practical charging application. The curve fitting was employed to model the equation between the charge current and the RSOC. The 4400 mAh battery pack (4S2P) was used in this study. Fig. 3 illustrates the dependence of the charge current on different RSOCs. The curve function fitted by the quadratic polynomial is expressed by

$$I_{SOC} = k_1 \cdot RSOC^2 + k_2 \cdot RSOC + k_3 \tag{1}$$

For the specification of the used battery pack, the coefficient k_1 is $-2.5 \cdot 10^{-4}$, k_2 is 0.001167, and k_3 is 3.74.

TABLE II. THE CT RATIO

SOC \ I_{ch}	0.2C	0.3C	0.4C	0.5C	0.6C	0.7C	0.8C	0.9C	1C
0%	0.33	0.46	0.57	0.68	0.76	0.84	0.89	0.95	1
10%	0.35	0.48	0.59	0.75	0.78	0.85	0.91	0.95	1
20%	0.37	0.50	0.61	0.72	0.79	0.86	0.92	0.93	1
30%	0.40	0.53	0.63	0.73	0.81	0.87	0.91	0.94	1
40%	0.41	0.55	0.72	0.76	0.82	0.89	0.92	0.95	1
50%	0.47	0.58	0.76	0.79	0.85	0.90	0.93	0.96	1
60%	0.49	0.63	0.75	0.82	0.87	0.92	0.94	0.96	1
70%	0.59	0.69	0.78	0.85	0.90	0.94	0.95	0.99	1
80%	0.63	0.76	0.83	0.91	0.92	0.98	0.98	0.98	1
90%	0.80	0.89	0.94	0.98	0.99	0.99	1.00	1.00	1

TABLE III. CORRESOPNDING CHARGE CURRENTS AS CT RATIO ABOVE 0.9

RSOC	0%	10%	20%	30%	40%
I_{ch} (A)	$I_1=0.9\times I_{bat}$	$I_2=0.8\times I_{bat}$	$I_3=0.8\times I_{bat}$	$I_3=0.8\times I_{bat}$	$I_4=0.8\times I_{bat}$
RSOC	50%	60%	70%	80%	90%
I_{ch} (A)	$I_5=0.7\times I_{bat}$	$I_6=0.7\times I_{bat}$	$I_7=0.6\times I_{bat}$	$I_8=0.5\times I_{bat}$	$I_9=0.4\times I_{bat}$

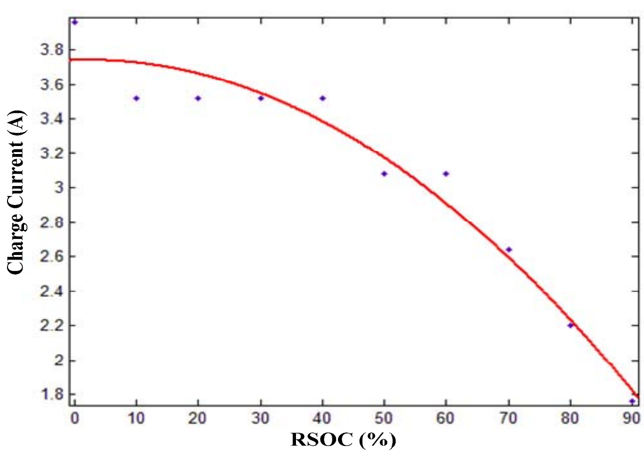

Fig. 3. Relation between charge current and RSOC and the fitting curve.

C. Fuzzy Temperature Controller

In order to mitigate the battery aging effect, a fuzzy temperature controller (FTC) is designed to fine modulate the charge current. This fine-tune current is added to the coarse-tuning charge current to produce an appropriate charge current, which features ability of temperature rise control. That is, an incremental current ΔI was generated by the FTC and added to the I_{SOC} to regulate the charge current according to the variation of the present operating temperature. When the temperature rise was increase during charging, the charging current I_{SOC} will be reduced for a ΔI step consecutively to drop the temperature rise and diminish impact on the battery. On the other hand, as the temperature rise was decreasing, the charging current will be increased for a ΔI step each time to speed up the CT.

The scheme of the proposed FTC is shown in Fig. 4. From Fig. 4, the input variables of the FTC are the temperature rise (DT) and the gradient of temperature rise (ΔDT). In which the DT was defined as the difference between the battery surface temperature and the room temperature. The ΔDT was the difference between the present DT and the DT before two seconds. The output variable was the incremental current ΔI., The Mamdani-type minimum inferential method cooperating with the center of sum (COS) defuzzification procedure was utilized in this paper to obtain the crisp output. The membership functions (MFs) corresponding to the DT, ΔDT, and ΔI are illustrated in Fig. 5(a)-(c), respectively. The universe of discourse (UOD) in the MFs of DT and ΔDT are defined on the domain [0ºC, 4ºC] and [-0.1ºC, 0.1ºC], respectively. The UOD of the output variable MF is defined on the domain [-20%, 20%]. In Fig. 5(a)-(c), the linguistic values TS, TMS, TM, TML, and TL represent temperature small, temperature medium small, temperature medium, temperature medium large, and temperature large, respectively. The dT_NL, dT_NS, dT_Z, dT_PS, and dT_PL stand for delta temperature negative large, delta temperature negative small, delta temperature zero, delta temperature positive small, and delta temperature positive large, respectively. The ΔI_NL, ΔI_NS, ΔI_Z, ΔI_PS, and ΔI_PL denote delta I negative large, delta I negative small, delta I zero, delta I positive small, and delta I positive large, respectively. According to the expert experience and knowledge base, the rule base of the incremental current ΔI are derived in Fig. 6. For example, the inference rule can be described as if DT is small and ΔDT is negative large, then the ΔI is positive large (Rule01). From Rule01, we know that the chemical reaction inside the battery was not severe and the temperature was low. Hence, the charging current can be increased to accelerate the charge time.

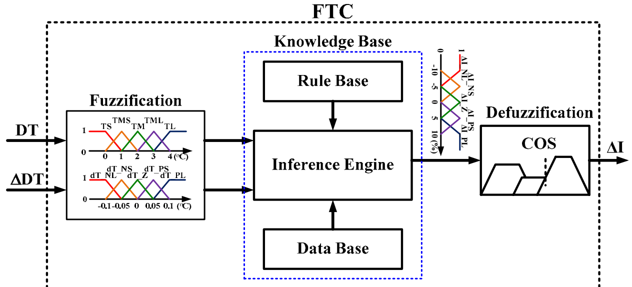

Fig. 4. Scheme of the FTC.

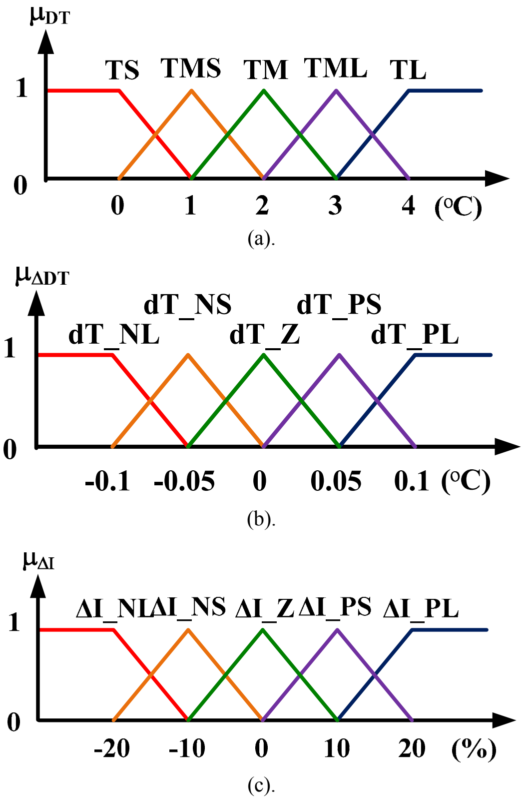

Fig. 5. MFs corresponding to (a) DT; (b) ΔDT; and (c) ΔI.

ΔDT \ DT	TS	TMS	TM	TML	TL
dT_NL	Rule01 ΔI_PL	Rule06 ΔI_PL	Rule11 ΔI_PS	Rule16 ΔI_Z	Rule21 ΔI_Z
dT_NS	Rule02 ΔI_PL	Rule07 ΔI_PS	Rule12 ΔI_PS	Rule17 ΔI_Z	Rule22 ΔI_NS
dT_Z	Rule03 ΔI_PS	Rule08 ΔI_PS	Rule13 ΔI_Z	Rule18 ΔI_NS	Rule23 ΔI_MS
dT_PS	Rule04 ΔI_Z	Rule09 ΔI_Z	Rule14 ΔI_NS	Rule19 ΔI_NS	Rule24 ΔI_NL
dT_PL	Rule05 ΔI_NS	Rule10 ΔI_NS	Rule15 ΔI_NL	Rule20 ΔI_NL	Rule25 ΔI_NL

Fig. 6. Rule base for ΔI.

III. Experimental Results

The measured waveforms were provided in this section to confirm the correctness and performance of the proposed charging strategy. In addition, the measured data obtained from the CC-CV, RC, and RC with FTC (FRC) were analyzed and compared to highlight the effectiveness of the studied method on temperature rise alleviation. Fig. 7 shows the user menu of the GUI and the measured data and waveforms. Two variable steps of the incremental current ΔI ($\Delta I_{10\%}$ and $\Delta I_{20\%}$) were studied for the proposed charging method to further check and clarify the effect of the temperature rise mitigation. Fig. 8 shows the measured charging currents for different charge methods. The variation of the temperature rise result from different charge methods was shown in Fig. 9. The maximum and average temperature rises for different charging methods were tabulated in Table IV.

From Fig. 8 and 9, under the control of the temperature rise suppression, we can see that the charging currents of the proposed FRC charge methods (for $\Delta I_{10\%}$ and $\Delta I_{20\%}$ steps) are less and have the smoother variation than those of the CC-CV and RC charge methods in spite of the charging terminated time is slightly longer than those of the counterpart methods. Accordingly, the proposed FRC with 20% ΔI step has the best suppressive effect on temperature rise and outperforms other methods. Furthermore, form Table IV, comparing the average temperature rise of the three studied methods (RC, FRC with $\Delta I_{10\%}$ and $\Delta I_{20\%}$) to that of the conventional CC-CV method, the average temperature rise has the reductions of 18.5%, 23.2% and 31.24%, respectively. On the other hand, due to the less temperature rise leads to the less power loss and aging effect. Therefore, the charging efficiency of the studied methods has the increases of 1.62%, 1.76% and 2.06% respectively when comparing with that of the conventional CC-CV method.

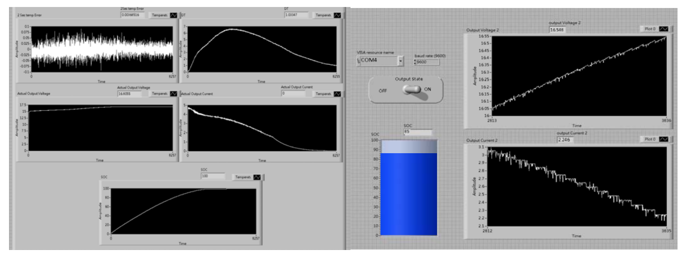

Fig. 7. The GUI and recording data.

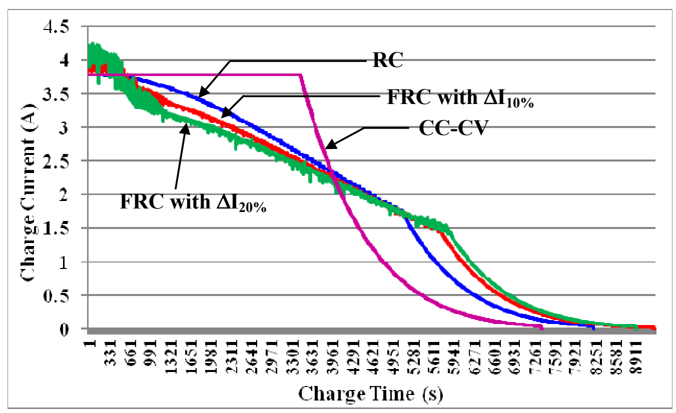

Fig. 8. Measured charge currents for different methods.

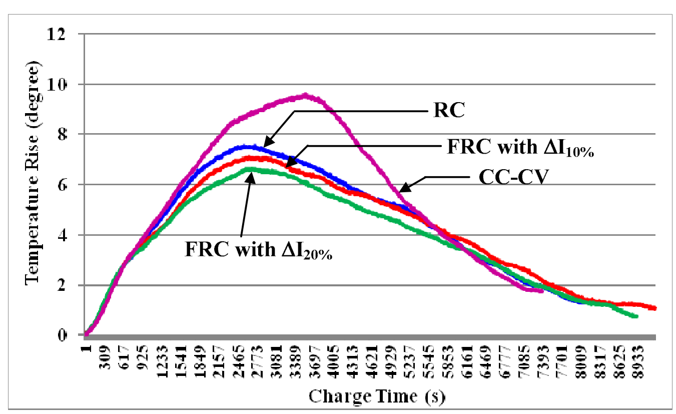

Fig. 9. Measured temperature rise for different methods.

TABLE IV. MAX. AND AVG. TR FOR VARIOUS METHODS

	CC-CV		RC		FRC with $\Delta I_{10\%}$		FRC with $\Delta I_{20\%}$	
Test no.	**Max. TR (ºC)**	**Avg. TR (ºC)**	**Max. TR (ºC)**	**Avg. TR (ºC)**	**Max. TR (ºC)**	**Avg. TR (ºC)**	**Max. TR (ºC)**	**Avg. TR (ºC)**
1	**9.382**	**5.451**	**7.328**	**4.550**	**7.232**	**4.338**	**6.634**	**3.879**
2	**9.567**	**5.547**	**6.954**	**4.454**	**7.081**	**4.231**	**6.310**	**3.661**
3	**9.495**	**5.551**	**7.527**	**4.480**	**6.857**	**4.140**	**6.500**	**3.839**
Avg.	**9.481**	**5.516**	**7.270**	**4.495**	**7.057**	**4.236**	**6.481**	**3.793**

IV. CONCLUSIONS

A digitally-controlled Li-ion battery charger has been studied and developed in this paper. The devised charger can dynamically generate the adaptive charging current depending on the battery SOC condition and temperature variation. Therefore, the battery and ambience temperatures have been considered in this study. Experimental results have shown that the proposed RC charge method with fuzzy temperature control can avoid using high C-rate current to charge high RSOC battery and aggravating battery aging due to the large stress of the electrochemical reaction.

The power stage of the proposed charger is implemented by the synchronous-rectified buck converter. The firmware and GUI of the proposed system were realized by the microcontroller unit and LabVIEW software. Experimental results validate the correctness and effectiveness of the proposed charger and control approach. The largest 23.2% reduction of the average temperature rise and the largest 2.06% boost of the charge efficiency have been achieved while maintaining similar charging time as comparing to the conventional CC-CV method. As a result, the proposed technique can dynamically provide the adaptive current to charge the battery according to the current SOC and ambience temperature variation. It also effectively improves the battery aging effect due to the large temperature rise and enhances the charging efficiency. .

ACKNOWLEDGMENT

This work was supported by the Ministry of Science and Technology of Taiwan under Grant MOST 104-2221-E-262-008.

REFERENCES

[1] L. Lam and P. Bauer, “Practical capacity fading model for Li-ion battery cells in electric vehicles,” *IEEE Trans. Power Electron.*, vol. 28 no. 12, pp. 5910-5918, Dec. 2013.

[2] S. Bhide and T. Shim, “Novel predictive electric Li-ion battery model incorporating thermal and rate factor effects,” *IEEE Trans. Veh. Technol.,* vol. 60, no. 3, pp. 819–829, Mar. 2011.

[3] B. D. Valle, C. T. Wentz, and R. Sarpeshkar, “An area and power-efficient analog Li-ion battery charger circuit,” *IEEE Trans. Biomed. Circuits Syst.,* vol. 5, no. 2, pp. 131–137, Apr. 2011.

[4] H. Rahimi-Eichi, F. Baronti, and M. Y. Chow, “Online adaptive parameter identification and state-of-charge coestimation for lithium-polymer battery cells,” *IEEE Trans. Ind. Electron.*, vol. 61, no. 4, pp. 2053–2061, Apr. 2014.

[5] S. Chae, Y. Song, S. Park, and H. Jeong, “Digital current sharing method for parallel interleaved DC–DC converters using input ripple voltage,” *IEEE Trans. Ind. Inf.*, vol. 8, no. 3, pp. 536-544, Aug. 2012.

[6] J. Jiang, Q. Liu, C. Zhang, and W. Zhangnd, “Evaluation of acceptable charging current of power Li-ion batteries based on polarization characteristics,” *IEEE Trans. Ind. Electron.*, vol. 61, no. 12, pp. 6844–6851, Dec. 2014.

[7] F. Hoffart, “Proper care extends Li-ion battery life,” *Power Electron. Technol. Mag.*, pp. 24–28, Apr. 2008.

[8] R. Pagano, M. Baker,and R. E. Radke, “A 0.18-μm monolithic Li-ion battery charger for wireless devices based on partial current sensing and adaptive reference voltage,” *IEEE J. Solid-State Circuits*, vol. 47, no. 6, pp. 1355–1368, Jun. 2012.

[9] L. R. Chen, C. S. Liu, J. J. Chen, “Improving phase-locked battery charger speed by using resistance-compensated technique,” *IEEE Trans. Ind. Electron.*, vol. 56, no. 4, pp. 1205-1211, Apr. 2009.

[10] L. R. Chen, “Design of duty-varied voltage pulse charger for improving Li-ion battery-charging response,” *IEEE Trans. Ind. Electron.*, vol. 56, no. 2, pp. 480-487, Feb. 2009.

[11] L. R. Chen, J. J. Chen, N. Y. Chu, and G. Y. Han, “Current-pumped battery charger,” *IEEE Trans. Ind. Electron.*, vol. 55, no. 6, pp. 2482–2488, Jun. 2008.

[12] L. R. Chen, “A design of an optimal battery pulse charge system by frequency-varied technique,” *IEEE Trans. Ind. Electron.*, vol. 54, no. 1, pp. 398–405, Feb. 2007.

[13] T. Ikeya, N. Sawada, S. Takagi, J. Murakami, and K. Kobayashi et al., “Multi-step constant-current charging method for electric vehicle, valve-regulated, lead/acid batteries during night time for load-leveling,” *J. Power Sources*, vol. 75, no. 1, pp. 101–107, Sept. 1998.

[14] T. Ikeyaa, N. Sawadab, J. I. Murakamic, K. Kobayashi, M. Hattori, N. Murotani, S. Ujiie, K. Kajiyama, H. Nasu, H. Narisoko, Y. Tomaki, K. Adachi, Y. Mita, and K. Ishihara, “Multi-step constant-current charging method for an electric vehicle nickel/metal hydride battery with high energy efficiency and long cycle life,” *J. Power Sources*, vol. 105, no. 1, pp. 6–12, 2002.

[15] J. W. Huang, Y, H. Liu, S. C. Wang, and Z. Z. Yang, “Fuzzy-control-based five-step Li-ion battery charger,” in *Proc. IEEE Int. Conf. PEDS*, Nov. 2009, pp. 1547–1551.

[16] F. J. Lin, M. S. Huang, P. Y. Yeh, H. C. Tsai, and C. H. Kuan, “DSP-based probabilistic fuzzy neural network control for Li-ion battery charger,” *IEEE Trans. Power Electron.*, vol. 27 no. 8, pp. 3782-3794, Aug. 2012.

[17] K. Thirugnanam, J.T.P. Ezhil Reena, M. Singh, and P. Kumar, “Mathematical modeling of Li-ion battery using genetic algorithm approach for V2G applications,” *IEEE Trans. Energy Convers.*, vol. 29, no. 2, pp. 332–343, Jun. 2014.

[18] S. C. Wang and Y. H. Liu, “A PSO-based fuzzy-controlled searching for the optimal charge pattern of Li-ion batteries,” *IEEE Trans. Ind. Electron.*, vol. 62, no. 5, pp. 2983-2993, May 2015.